Hindawi Publishing Corporation
Mathematical Problems in Engineering
Volume 2016, Article ID 3986903, 9 pages
http://dx.doi.org/10.1155/2016/3986903

Research Article

A Novel STAP Algorithm for Airborne MIMO Radar Based on Temporally Correlated Multiple Sparse Bayesian Learning

Hanwei Liu,[1] Yongshun Zhang,[1] Yiduo Guo,[1] Qiang Wang,[1] and Yifeng Wu[2]

[1]*Air Force Engineering University, Xi'an 710051, China*
[2]*National Laboratory of Radar Signal Processing, Xidian University, Xi'an 710071, China*

Correspondence should be addressed to Hanwei Liu; liuhanwei_12345@163.com

Received 1 March 2016; Revised 28 June 2016; Accepted 20 July 2016

Academic Editor: Cornel Ioana

In a heterogeneous environment, to efficiently suppress clutter with only one snapshot, a novel STAP algorithm for multiple-input multiple-output (MIMO) radar based on sparse representation, referred to as MIMOSR-STAP in this paper, is presented. By exploiting the waveform diversity of MIMO radar, each snapshot at the tested range cell can be transformed into multisnapshots for the phased array radar, which can estimate the high-resolution space-time spectrum by using multiple measurement vectors (MMV) technique. The proposed approach is effective in estimating the spectrum by utilizing Temporally Correlated Multiple Sparse Bayesian Learning (TMSBL). In the sequel, the clutter covariance matrix (CCM) and the corresponding adaptive weight vector can be efficiently obtained. MIMOSR-STAP enjoys high accuracy and robustness so that it can achieve better performance of output signal-to-clutter-plus-noise ratio (SCNR) and minimum detectable velocity (MDV) than the single measurement vector sparse representation methods in the literature. Thus, MIMOSR-STAP can deal with badly inhomogeneous clutter scenario more effectively, especially suitable for insufficient independent and identically distributed (IID) samples environment.

1. Introduction

Space-time adaptive processing (STAP) is a crucial technique which is used in airborne phased array radar to suppress clutter for target detection [1]. However, the fully adaptive STAP processor is difficult to be applied in practice, due to the lack of sufficient independent and identically distributed (IID) training samples in seriously nonhomogeneous environment. Focused on nonhomogeneous clutter scenario, many strategies have been proposed [2–8], that is, STAP algorithms based on reduce-dimension (RD), reduce-rank (RR), direct data domain (DDD), and space-time autoregressive filtering (STAR). However, the abovementioned methods' clutter covariance matrix based on maximum-likelihood estimation, called traditional STAP methods, requires twice the degree of freedom (DOF) of IID training samples if it is intended to acquire less than 3 dB loss of optimal performance [9]. Ginolhac et al. [7, 8] proposed a new LR-STAP filter by cleverly taking into account the persymmetric structure of the noise covariance matrix (CM) and the low-rank (LR) structure of the clutter. The resulting STAP filter is shown, both theoretically and experimentally, to exhibit 3 dB SINR loss performance with only r secondary data (where r is the clutter rank). The IID training samples support can be further reduced. Thus, it can be seen that reducing the number of secondary data used to estimate the CM for STAP technique is still an active research topic.

Inspired by the rapid development of sparse representation (SR) and compressed sensing (CS) theory, clutter covariance matrix (CCM) can be estimated by utilizing SR technique [10, 11] which needs much fewer training samples compared with traditional STAP methods, and it is referred to as SR-STAP in [10–12]. However, using the data of single snapshot in SR-STAP [12] may lead to estimation errors, such as clutter spectrum disconnection and "pseudopeaks." Hence, to prevent a potential sacrifice of sparse representation performance happening and make sufficient use of the adjacent multiple snapshots, it would better transform from the single measurement vector (SMV) sparse solution problem into the multiple measurement vectors (MMV) joint

sparse solution problem. The MMV problem caught many scholars' attention [11]. Moreover, to suppress the seriously heterogeneous clutter, direct data domain (D3) method has been proposed. In [13], owing to the intrinsic sparsity of the spectral distribution, a new direct data domain approach is examined, which seeks to estimate the high-resolution spectrum by using focal underdetermined system solution (FOCUSS) and L1 norm minimization. In [10], by exploiting the space-time smoothing techniques, one snapshot of the cell under test (CUT) generates multiple subsnapshots. And then, the angle-Doppler profile is estimated by using the least absolute shrinkage and selection operator (LASSO) solution.

However, there are two problems in view of the aforementioned facts. Firstly, the stationarity is hard to be guaranteed; for example, short-range clutter environment in non-side-looking airborne radar is seriously nonhomogeneous, which results in clutter distribution varying with range and training samples in different range cell unsatisfying IID. Conventional SR-STAP cannot be used. Secondly, the accuracy of clutter space-time spectrum estimation has a great impact on the clutter suppression performance, and the calculation error due to sparse recovery in noise background should be further reduced. To resolve the above issues, a novel STAP algorithm for airborne MIMO radar based on Temporally Correlated Multiple Sparse Bayesian Learning is proposed, which can effectively suppress clutter with only one snapshot. The proposed method maintains further accuracy and robustness to noise so that it can achieve better performance of output signal-to-clutter ratio (SCR) and minimum detectable velocity (MDV) than current single measurement vector sparse representation.

The rest of the paper is organized as follows. The principle of SR-STAP is briefly introduced and the signal model of the problem is formulated in Section 2. In Section 3, multiple snapshot generation is studied. Then, the novel STAP algorithm for airborne MIMO radar is proposed to mitigate the strong ground clutter based on Temporally Correlated Multiple Sparse Bayesian Learning (TMSBL). In Section 4, simulation results are provided to assess the effectiveness of the proposed method. Finally, conclusions are presented in Section 5.

2. Principle of SR-STAP and Problem Formulation

In airborne radar systems, ignoring the range ambiguity, a general model of the space-time clutter plus noise can be expressed as

$$\mathbf{x} = \mathbf{x}_c + \mathbf{n} = \sum_{i=1}^{N_c} \rho_i \mathbf{v}\left(f_{di}, f_{si}\right) + \mathbf{n}, \tag{1}$$

where $\mathbf{n}$ is the Gaussian white noise vector, N_c is the number of independent clutter patches that are evenly distributed in azimuth, and ρ_i, f_{si}, and f_{di} are the complex-valued scattering coefficient, spatial frequency, and Doppler frequency of the ith clutter patch, respectively. $\mathbf{v}(f_{di}, f_{si})$ is the $NK \times 1$ space-time steering vector, and it is given by

$$\mathbf{v}\left(f_{di}, f_{si}\right) = \left[1, \ldots, e^{j2\pi(N-1)f_{si}}, e^{j2\pi f_{di}}, \ldots, e^{j2\pi((K-1)f_{di}+(N-1)f_{si})}\right]^T. \tag{2}$$

The whole angle-Doppler plane is discretized into $N_s \times N_d$ grids, where $N_s = \eta_s N$ and $N_d = \eta_d N$ (η_s and η_d denote the resolution) are the number of angle and Doppler bins, respectively. Afterwards, the received signal in (1) can be rewritten as

$$\mathbf{x} = \mathbf{\Phi}\boldsymbol{\gamma} + \mathbf{n}, \tag{3}$$

where $\mathbf{\Phi} = [\mathbf{v}(f_{d1}, f_{s1}), \ldots, \mathbf{v}(f_{d1}, f_{sN_s}), \ldots, \mathbf{v}(f_{dN_d}, f_{sN_s})] \in \mathbb{C}^{NK \times N_d N_s}$ is the redundant space-time completed dictionary and $\boldsymbol{\gamma} = [\gamma(1,1), \ldots, \gamma(1,N_s), \ldots, \gamma(N_d, N_s)]^T \in \mathbb{C}^{N_s N_d \times 1}$ is the angle-Doppler profile with nonzero elements representing the clutter.

According to [14–16], solving (3) for its sparse solution can be transformed to $L0$ optimization problem as follows:

$$\begin{aligned} \min \quad & \|\boldsymbol{\gamma}\|_0, \\ \text{s.t.} \quad & \|\mathbf{x} - \mathbf{\Phi}\boldsymbol{\gamma}\|_2 \le \varepsilon. \end{aligned} \tag{4}$$

As to (4), it has been proven to be an NP-hard problem. Fortunately, by $L1$ optimization, we could find the solution of (4) with some characteristic of sparsity. There are a lot of algorithms to solve this type of problem [17–19], such as OMP algorithm [17], FOCUSS algorithm [18], and SBL algorithm [19].

Based on the above discussion, the clutter covariance matrix can be estimated by

$$\mathbf{R}_{\mathrm{SR}} = \sum_{i=1}^{N_d} \sum_{j=1}^{N_s} \left|\gamma(i,j)\right|^2 \mathbf{v}\left(f_{di}, f_{sj}\right) \mathbf{v}^H\left(f_{di}, f_{sj}\right) + \sigma^2 \mathbf{I}, \tag{5}$$

where σ^2 is the noise power and $\mathbf{I}$ denotes the identity matrix. As the estimated clutter space-time spectrum $\boldsymbol{\gamma}$ is not stable with only one snapshot, CCM estimation is inaccurate and the clutter suppression performance degrades significantly. To make sufficient use of the multiple snapshots and obtain a better clutter suppression performance, multisnapshots are employed in synergy, which is called sparse solution with multiple measurement vectors [20–22] (MMV). As stated in [11], selecting L IID training range cells from both sides of the cell under test, (3) can be rewritten by

$$\mathbf{X} = \mathbf{\Phi}\mathbf{\Upsilon} + \mathbf{N}, \tag{6}$$

where $\mathbf{X} = [\mathbf{x}_1, \mathbf{x}_2, \ldots, \mathbf{x}_L] \in \mathbb{C}^{NK \times L}$, $\mathbf{\Upsilon} = [\boldsymbol{\gamma}_1, \boldsymbol{\gamma}_2, \ldots, \boldsymbol{\gamma}_L] \in \mathbb{C}^{N_s N_d \times L}$, and $\mathbf{N} = [\mathbf{n}_1, \mathbf{n}_2, \ldots, \mathbf{n}_L] \in \mathbb{C}^{NK \times L}$. The estimated clutter space-time spectrum can be obtained as $\overline{\mathbf{\Upsilon}} = \sum_{l=1}^{L} \boldsymbol{\gamma}_l / L$. The clutter covariance matrix can be estimated by (5).

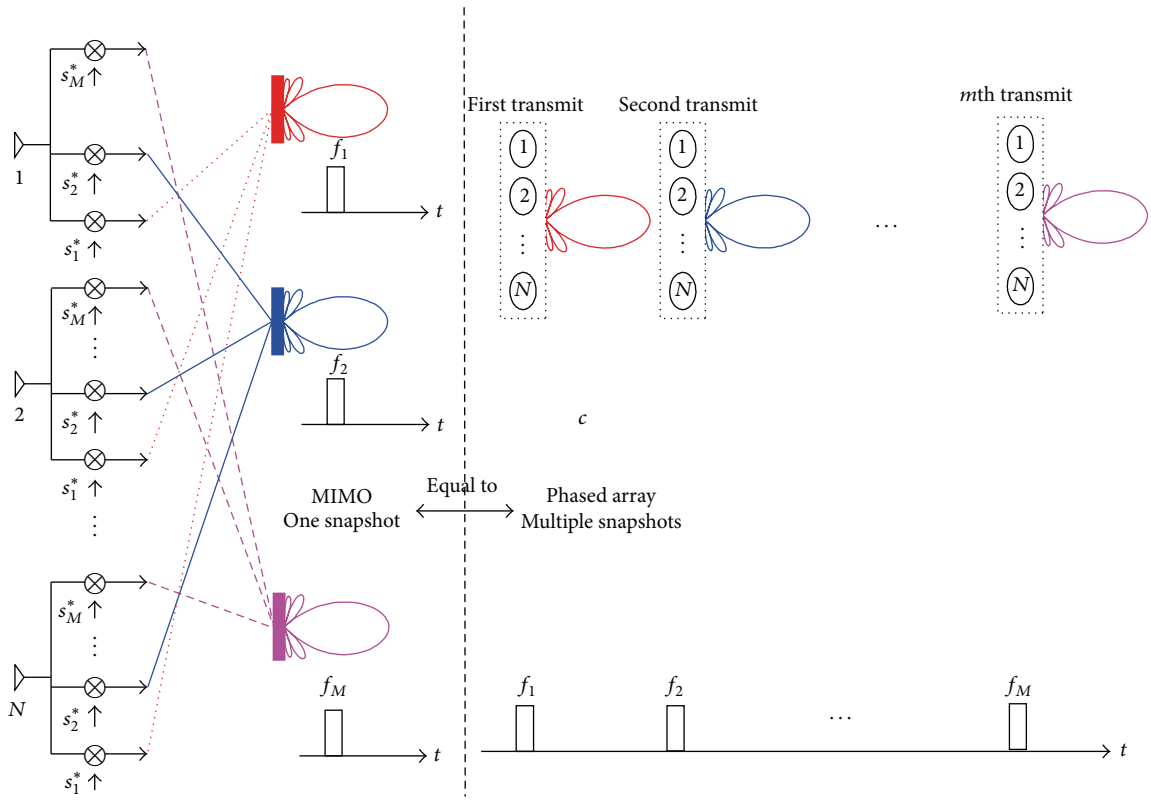

FIGURE 1: Cell under test transformed into multisnapshots.

Finally, the weight vector of STAP processor can be calculated by

$$\mathbf{w}_{\mathrm{SR}} = \mathbf{R}_{\mathrm{SR}}^{-1}\mathbf{v}\left(f_{dt}, f_{st}\right), \tag{7}$$

where $\mathbf{v}(f_{dt}, f_{st})$ is the space-time steering vector of target.

The calculation error may be serious in the procedure of sparse representation for STAP, because the single selected snapshot contains random noise and clutter. Utilizing multiple IID snapshots improves the robustness of the method. However, IID samples are difficult to acquire in seriously nonhomogeneous clutter environment.

3. MIMOSR-STAP Method Based on TMSBL

MIMO radar has the superiority of waveform diversity and increases the dimension of receiving data. A novel STAP algorithm for airborne MIMO radar based on TMSBL is presented in this section. The single snapshot of range cell data in MIMO radar can be equivalent to multiple snapshots data in conventional phased array radar. The procedure of multiple snapshot generation is shown in Figure 1, and the method is described in detail as follows.

3.1. Multiple Snapshot Generation. Without loss of generality, we consider the side-looking MIMO radar with collocated transmit and receive arrays. The transmit and receive arrays are both uniform linear array with M and N elements, respectively. K pulses are transmitted during the coherent processing interval. The transmitted waveforms are assumed to be orthogonal. In the receive array, the received echoes are downconverted, match-filtered, and stored. For each receive antenna and pulse, the received signal can be decomposed by M matched filters, yielding M isolated waveforms. After match-filtering, the output of the mth transmit element, nth receive element, and kth pulse is

$$\begin{aligned} r_{m,n,k} = \xi \exp&\left\{\frac{j2\pi\left(m-1\right)d_T \sin\theta}{\lambda}\right\} \\ &\cdot \exp\left\{\frac{j2\pi\left(n-1\right)d_R \sin\theta}{\lambda}\right\} \\ &\cdot \exp\left\{j2\pi\left(k-1\right)f_d T\right\}, \end{aligned} \tag{8}$$

where ξ is the amplitude of the received signal. $f_d = 2[v_a \cos\psi + v]/\lambda$ is the Doppler frequency of the target and v_a and v are the velocities of the platform and moving target. T is the pulse repetition interval (PRI). By exploiting the waveform diversity of MIMO radar, the cell under test can be transformed into multisnapshots for phased array radar, which seeks to estimate the high-resolution space-time spectrum with multiple measurement vectors.

As shown in Figure 1, the received target data in transmit-receive-time dimensions can be rearranged as

$$\mathbf{X}_{\text{tar}} = \begin{bmatrix} r_{1,1,1} & r_{2,1,1} & \cdots & r_{M,1,1} \\ r_{1,2,1} & r_{2,2,1} & \cdots & r_{M,2,1} \\ \vdots & \vdots & & \vdots \\ r_{1,N,1} & r_{2,N,1} & \cdots & r_{M,N,1} \\ r_{1,1,2} & r_{2,1,2} & \cdots & r_{M,1,2} \\ r_{1,2,2} & r_{2,2,2} & \cdots & r_{M,2,2} \\ \vdots & \vdots & & \vdots \\ r_{1,N,K} & r_{2,N,K} & \cdots & r_{M,N,K} \end{bmatrix}, \tag{9}$$

$$\begin{aligned} \mathbf{X}_{\text{tar}} &= \left[\mathbf{x}_{\text{tar\_1}}, \mathbf{x}_{\text{tar\_2}}, \ldots, \mathbf{x}_{\text{tar\_}m}, \ldots, \mathbf{x}_{\text{tar\_}M}\right] \in \mathbb{C}^{NK\times M}, \\ \mathbf{x}_{\text{tar\_}m} &= \left[r_{m,1,1}, r_{m,2,1}, \ldots, r_{m,N,1}, \ldots, r_{m,N,K}\right]^T \\ &= \xi \exp\left\{\frac{j2\pi (m-1) d_T \sin\theta}{\lambda}\right\} \mathbf{S}_t(v) \otimes \mathbf{S}_{\text{sr}}(\theta) \\ &= \sigma_{t,m} \mathbf{v}\left(f_{dt}, f_{st}\right), \end{aligned}$$

where $\otimes$ is the Kronecker product and $\mathbf{S}_t(v) \in \mathbb{C}^{K\times 1}$ and $\mathbf{S}_{\text{sr}}(\theta) \in \mathbb{C}^{N\times 1}$ are the Doppler steering vector and received steering vectors, respectively, and they have the following forms:

$$\begin{aligned} \mathbf{S}_t(v) &= \left[1, \exp\left(j4\pi \frac{v_a \sin\theta + v}{\lambda fr}\right), \ldots, \right. \\ &\qquad \left. \exp\left(j4\pi (K-1) \frac{v_a \sin\theta + v}{\lambda fr}\right)\right]^T, \\ \mathbf{S}_{\text{sr}}(\theta) &= \left[1, \exp\left(\frac{j2\pi d_R \sin\theta}{\lambda}\right), \ldots, \right. \\ &\qquad \left. \exp\left(\frac{j2\pi (N-1) d_R \sin\theta}{\lambda}\right)\right]^T. \end{aligned} \tag{10}$$

For airborne radar, the ground clutter echo corresponding to a particular range bin results from coherent summation of numerous statistically independent clutter patches over the iso-range. The clutter is given by

$$\begin{aligned} \mathbf{X}_{\text{clu}} &= \left[\mathbf{x}_{\text{clu\_1}}, \mathbf{x}_{\text{clu\_2}}, \ldots, \mathbf{x}_{\text{clu\_}m}, \ldots, \mathbf{x}_{\text{clu\_}M}\right] \in \mathbb{C}^{NK\times M}, \\ \mathbf{x}_{\text{clu\_}m} &= \sum_{i=1}^{N_c} \xi_i \exp\left\{\frac{j2\pi\alpha (m-1) d_R \sin\theta_i}{\lambda}\right\} \mathbf{S}_t(0) \otimes \mathbf{S}_{\text{sr}}(\theta_i) \\ &= \sum_{i=1}^{N_c} \sigma_{i,m} \mathbf{v}\left(f_{di}, f_{si}\right), \end{aligned} \tag{11}$$

where ξ_i denotes complex-valued scattering coefficient of the ith clutter patch and N_c is the number of independent clutter sources that are evenly distributed in azimuth.

Consequently, the space-time snapshot of the cell under test can be expressed as $NK \times M$ dimensional matrix:

$$\begin{aligned} \mathbf{X} &= \left[\mathbf{x}_1, \mathbf{x}_2, \ldots, \mathbf{x}_m, \ldots, \mathbf{x}_M\right] = \mathbf{X}_{\text{tar}} + \mathbf{X}_{\text{clu}} + \mathbf{X}_n \\ &\quad \in \mathbb{C}^{NK\times M}, \\ \mathbf{x}_m &= \mathbf{x}_{\text{tar\_}m} + \mathbf{x}_{\text{clu\_}m} + \mathbf{n}_m \\ &= \sum_{i=1}^{N_c} \sigma_{i,m} \mathbf{v}\left(f_{di}, f_{si}\right) + \sigma_{t,m} \mathbf{v}\left(f_{dt}, f_{st}\right) + \mathbf{n}_m, \end{aligned} \tag{12}$$

where $\sigma_{t,m} = \xi \exp\{j2\pi\alpha(m-1)d_R \sin\theta/\lambda\}$ and $\sigma_{i,m} = \xi_i \exp\{j2\pi\alpha(m-1)d_R \sin\theta_i/\lambda\}$ are the amplitudes of the target and the ith clutter patch corresponding to the mth transmit waveform. ξ denotes the scattering coefficient of the target and ξ_i denotes the scattering coefficient of the ith patch.

As stated in (3), the received data of the mth transmit waveform at CUT can be expressed as

$$\mathbf{x}_m = \sum_{i=1}^{N_s} \sum_{j=1}^{N_d} \gamma_m(i,j)\, v\left(f_{di}, f_{sj}\right) + \mathbf{n}_m = \boldsymbol{\Phi}\boldsymbol{\gamma}_m + \mathbf{n}_m, \tag{13}$$

where $\boldsymbol{\gamma}_m$ is the target and clutter space-time spectrum of the mth transmit waveform at CUT.

As M transmit waveforms have similar clutter structure, multisnapshots can be employed; that is,

$$\mathbf{X} = \boldsymbol{\Phi}\boldsymbol{\Upsilon} + \mathbf{N}, \tag{14}$$

where $\mathbf{X} = [\mathbf{x}_1, \mathbf{x}_2, \ldots, \mathbf{x}_M] \in \mathbb{C}^{NK\times M}$, $\boldsymbol{\Upsilon} = [\boldsymbol{\gamma}_1, \boldsymbol{\gamma}_2, \ldots, \boldsymbol{\gamma}_M] \in \mathbb{C}^{N_s N_d \times M}$, and $\mathbf{N} = [\mathbf{n}_1, \mathbf{n}_2, \ldots, \mathbf{n}_M] \in \mathbb{C}^{NK\times M}$.

3.2. STAP via TMSBL Algorithm. By employing the guidelines of the BCS approach in [23] for dealing with complex data, (14) can be rewritten as

$$\begin{bmatrix} \text{Re}(\mathbf{X}) \\ \text{Im}(\mathbf{X}) \end{bmatrix} = \begin{bmatrix} \text{Re}(\boldsymbol{\Phi}) & -\text{Im}(\boldsymbol{\Phi}) \\ \text{Im}(\boldsymbol{\Phi}) & \text{Re}(\boldsymbol{\Phi}) \end{bmatrix} \begin{bmatrix} \text{Re}(\boldsymbol{\Upsilon}) \\ \text{Im}(\boldsymbol{\Upsilon}) \end{bmatrix} + \begin{bmatrix} \text{Re}(\mathbf{N}) \\ \text{Im}(\mathbf{N}) \end{bmatrix}. \tag{15}$$

Re( ) and Im( ) are the operations that extract the real part and imaginary part from the complex number, respectively. Denote

$$\begin{aligned} \widehat{\mathbf{X}} &= \left[\text{Re}(\mathbf{X}) \;\; \text{Im}(\mathbf{X})\right]^T, \\ \widehat{\boldsymbol{\Phi}} &= \begin{bmatrix} \text{Re}(\boldsymbol{\Phi}) & -\text{Im}(\boldsymbol{\Phi}) \\ \text{Im}(\boldsymbol{\Phi}) & \text{Re}(\boldsymbol{\Phi}) \end{bmatrix}, \end{aligned} \tag{16}$$

$$\begin{aligned} \widehat{\boldsymbol{\Upsilon}} &= \left[\text{Re}(\boldsymbol{\Upsilon}) \;\; \text{Im}(\boldsymbol{\Upsilon})\right]^T, \\ \widehat{\mathbf{N}} &= \left[\text{Re}(\mathbf{N}) \;\; \text{Im}(\mathbf{N})\right]^T. \end{aligned} \tag{17}$$

And (15) can be rewritten as

$$\widehat{\mathbf{X}} = \widehat{\boldsymbol{\Phi}}\widehat{\boldsymbol{\Upsilon}} + \widehat{\mathbf{N}}. \tag{18}$$

Assume that the nth row of $\widehat{\mathbf{\Upsilon}}$ is mutually independent and each has a Gaussian distribution, given by

$$p\left(\widehat{\boldsymbol{\gamma}}_{n\cdot};\rho_n,\mathbf{B}_n\right)\sim N\left(\mathbf{0},\rho_n\mathbf{B}_n\right),\quad n=1,\ldots,2N_sN_d, \tag{19}$$

where ρ_n is an unknown variance parameter controlling the row sparsity in $\widehat{\mathbf{\Upsilon}}$ and $\mathbf{B}_n$ is a positive definite matrix that captures the temporal correlation of $\widehat{\boldsymbol{\gamma}}_n$. We reexpress (18) in vector form:

$$\mathbf{y}=\mathbf{\Psi}\mathbf{x}+\mathbf{v}, \tag{20}$$

where $\mathbf{y}=\mathrm{vec}(\widehat{\mathbf{X}}^T)\in\mathbb{C}^{2N_sN_dM\times 1}$, $\mathbf{\Psi}=\widehat{\mathbf{\Phi}}\otimes\mathbf{I}_M$, $\mathbf{x}=\mathrm{vec}(\widehat{\mathbf{\Upsilon}}^T)\in\mathbb{C}^{2N_sN_dM\times 1}$, and $\mathbf{v}=\mathrm{vec}(\widehat{\mathbf{N}}^T)\in\mathbb{C}^{2N_sN_dM\times 1}$. Suppose that the noise units in vector $\mathbf{v}$ are independent and each one is Gaussian with noise variance λ. Then, the Gaussian likelihood of (20) is given by

$$p\left(\mathbf{y}\mid\mathbf{x},\lambda\right)\sim N_{\mathbf{y}|\mathbf{x}}\left(\mathbf{\Psi}\mathbf{x},\lambda\mathbf{I}\right). \tag{21}$$

The prior distribution $\mathbf{x}$ of joint sparsity can be represented in vector form as follows:

$$p\left(\mathbf{x};\rho_n,\mathbf{B}_n\right)\sim N_{\mathbf{x}}\left(\mathbf{0},\mathbf{\Gamma}\otimes\mathbf{B}\right), \tag{22}$$

where $\mathbf{\Gamma}=\mathrm{diag}(\rho_1,\ldots,\rho_{2N_sN_d})$ and $\mathbf{B}=\mathrm{diag}(\mathbf{B}_1,\ldots,\mathbf{B}_{2N_sN_d})$. By combining the likelihood and the prior for x above, we can get the posterior density of $\mathbf{x}$ which is also Gaussian:

$$p\left(\mathbf{x}\mid\mathbf{y};\lambda,\rho_n,\mathbf{B}_n\right)\sim N_{\mathbf{x}}\left(\boldsymbol{\mu}_{\mathbf{x}},\mathbf{\Sigma}_{\mathbf{x}}\right), \tag{23}$$

where

$$\boldsymbol{\mu}_{\mathbf{x}}=\frac{\mathbf{\Sigma}_{\mathbf{x}}\mathbf{\Psi}^T\mathbf{y}}{\lambda}, \tag{24}$$

$$\mathbf{\Sigma}_{\mathbf{x}}=\left[\left(\mathbf{\Gamma}\otimes\mathbf{B}\right)^{-1}+\frac{\mathbf{\Psi}^T\mathbf{\Psi}}{\lambda}\right]^{-1}. \tag{25}$$

Using definition (25), the maximum a posteriori (MAP) estimate of $\mathbf{x}$ is given by

$$\begin{aligned}\mathbf{x}^*\triangleq\boldsymbol{\mu}_{\mathbf{x}}&=\left[\lambda\left(\mathbf{\Gamma}\otimes\mathbf{B}\right)^{-1}+\mathbf{\Psi}^T\mathbf{\Psi}\right]^{-1}\mathbf{\Psi}^T\mathbf{y}\\&=\left(\mathbf{\Gamma}\otimes\mathbf{B}\right)\mathbf{\Psi}^T\left[\lambda\mathbf{I}+\mathbf{\Psi}\left(\mathbf{\Gamma}\otimes\mathbf{B}\right)\mathbf{\Psi}^T\right]^{-1}\mathbf{y},\end{aligned} \tag{26}$$

where the last equation follows the matrix identity $(\mathbf{I}+\mathbf{AB})^{-1}\mathbf{A}=\mathbf{A}(\mathbf{I}+\mathbf{BA})^{-1}$. With a reasonable approximation $[\lambda\mathbf{I}+\mathbf{\Psi}(\mathbf{\Gamma}\otimes\mathbf{B})\mathbf{\Psi}^T]^{-1}\approx(\lambda\mathbf{I}+\widehat{\mathbf{\Phi}}\mathbf{\Gamma}\widehat{\mathbf{\Phi}}^T)^{-1}\otimes\mathbf{B}^{-1}$ [20] and $\mathbf{\Psi}=\widehat{\mathbf{\Phi}}\otimes\mathbf{I}_M$, (26) can be derived as

$$\begin{aligned}\mathbf{x}^*\triangleq\boldsymbol{\mu}_{\mathbf{x}}&\approx\left(\mathbf{\Gamma}\otimes\mathbf{B}\right)\left(\widehat{\mathbf{\Phi}}\otimes\mathbf{I}_M\right)^T\left[\left(\lambda\mathbf{I}+\widehat{\mathbf{\Phi}}\mathbf{\Gamma}\widehat{\mathbf{\Phi}}^T\right)^{-1}\otimes\mathbf{B}^{-1}\right]\mathbf{y}\\&=\left[\mathbf{\Gamma}\widehat{\mathbf{\Phi}}^T\left(\lambda\mathbf{I}+\widehat{\mathbf{\Phi}}\mathbf{\Gamma}\widehat{\mathbf{\Phi}}^T\right)^{-1}\otimes\mathbf{I}\right]\mathbf{y}.\end{aligned} \tag{27}$$

Equation (27) can be rewritten in a matrix form as follows:

$$\widehat{\mathbf{\Upsilon}}=\mathbf{\Gamma}\widehat{\mathbf{\Phi}}^T\left(\lambda\mathbf{I}+\widehat{\mathbf{\Phi}}\mathbf{\Gamma}\widehat{\mathbf{\Phi}}^T\right)^{-1}\widehat{\mathbf{X}}. \tag{28}$$

With the same approximation as above, (25) can be derived as follows:

$$\begin{aligned}\mathbf{\Sigma}_{\mathbf{x}}&=\left[\left(\mathbf{\Gamma}\otimes\mathbf{B}\right)^{-1}+\frac{\mathbf{\Psi}^T\mathbf{\Psi}}{\lambda}\right]^{-1}=\left(\mathbf{\Gamma}\otimes\mathbf{B}\right)-\left(\mathbf{\Gamma}\otimes\mathbf{B}\right)\\&\cdot\left(\mathbf{\Psi}^T\otimes\mathbf{I}\right)\left(\lambda\mathbf{I}+\mathbf{\Psi}\left(\mathbf{\Gamma}\otimes\mathbf{B}\right)\mathbf{\Psi}^T\right)^{-1}\left(\mathbf{\Psi}\otimes\mathbf{I}\right)\left(\mathbf{\Gamma}\otimes\mathbf{B}\right)\\&\approx\left(\mathbf{\Gamma}\otimes\mathbf{B}\right)-\left(\left(\mathbf{\Gamma}\widehat{\mathbf{\Phi}}^T\right)\otimes\mathbf{B}\right)\\&\cdot\left[\left(\lambda\mathbf{I}+\widehat{\mathbf{\Phi}}\mathbf{\Gamma}\widehat{\mathbf{\Phi}}^T\right)^{-1}\otimes\mathbf{B}^{-1}\right]\cdot\left(\left(\widehat{\mathbf{\Phi}}\mathbf{\Gamma}\right)\otimes\mathbf{B}\right)\\&=\left(\mathbf{\Gamma}-\mathbf{\Gamma}\widehat{\mathbf{\Phi}}^T\left(\lambda\mathbf{I}+\widehat{\mathbf{\Phi}}\mathbf{\Gamma}\widehat{\mathbf{\Phi}}^T\right)^{-1}\widehat{\mathbf{\Phi}}\mathbf{\Gamma}\right)\otimes\mathbf{B}\\&=\left(\mathbf{\Gamma}^{-1}+\frac{\widehat{\mathbf{\Phi}}^T\widehat{\mathbf{\Phi}}}{\lambda}\right)^{-1}\otimes\mathbf{B}=\mathbf{\Xi}_x\otimes\mathbf{B},\end{aligned} \tag{29}$$

where

$$\mathbf{\Xi}_x=\left(\mathbf{\Gamma}^{-1}+\frac{\widehat{\mathbf{\Phi}}^T\widehat{\mathbf{\Phi}}}{\lambda}\right)^{-1}. \tag{30}$$

Hyperparameters λ, $\mathbf{\Gamma}$, and $\mathbf{B}$ can be estimated with *Type II* maximum likelihood which is marginalized over the weights and then performs the maximum-likelihood estimation. For convenience, we list the estimated results derived in [20] as

$$\begin{aligned}\rho_n&=\frac{1}{M}\left(\widehat{\mathbf{X}}_{n\cdot}^T\mathbf{B}^{-1}\widehat{\mathbf{X}}_{n\cdot}+\left(\mathbf{\Xi}_x\right)_{nn}\right),\\\lambda&=\frac{\left\|\widehat{\mathbf{\Upsilon}}-\widehat{\mathbf{\Phi}}\widehat{\mathbf{X}}\right\|_F^2}{2N_sN_dM}+\frac{\lambda\,\mathrm{tr}\left[\widehat{\mathbf{\Phi}}\mathbf{\Gamma}\widehat{\mathbf{\Phi}}^T\left(\lambda\mathbf{I}+\widehat{\mathbf{\Phi}}\mathbf{\Gamma}\widehat{\mathbf{\Phi}}^T\right)^{-1}\right]}{2N_sN_d},\\\mathbf{B}&=\frac{\widetilde{\mathbf{B}}}{\left\|\widetilde{\mathbf{B}}\right\|_F},\quad\text{where }\widetilde{\mathbf{B}}=\sum_{n=1}^{2N_sN_d}\frac{\widehat{\mathbf{X}}_{n\cdot}^T\widehat{\mathbf{X}}_{n\cdot}}{\rho_n}.\end{aligned} \tag{31}$$

An iterative procedure is produced by the learning rules (28), (29), and (31), with which all hyperparameters can be estimated and the maximum a posteriori (MAP) estimate of $\widehat{\boldsymbol{\gamma}}$ can be obtained too. And then, $\boldsymbol{\gamma}=[\boldsymbol{\gamma}_1,\boldsymbol{\gamma}_2,\ldots,\boldsymbol{\gamma}_M]\in\mathbb{C}^{N_sN_d\times M}$ can be derived based on formula (17). Finally, the expected high-resolution space-time spectrum of target and clutter can be estimated by the algorithm mentioned above; the clutter distribution can be extracted using the assumed signal of interest (SOI), which follows a similar idea of D3 STAP method. Then, the CCM and the corresponding weight vector can be calculated by

$$\begin{aligned}\mathbf{R}_{\mathrm{SR}}&=\sum_{p=1}^{N_d}\sum_{q=1}^{N_s}\left|\overline{\boldsymbol{\gamma}}(p,q)\right|^2\boldsymbol{\phi}\left(f_{dp},f_{sq}\right)\boldsymbol{\phi}^H\left(f_{dp},f_{sq}\right)\\&\quad+\sigma^2\mathbf{I}_{NK},\quad(p,q)\notin\mathbf{\Omega}\left(f_{st},f_{dt}\right),\end{aligned} \tag{32}$$

$$\mathbf{w}_{\mathrm{SR}}=\mathbf{R}_{\mathrm{SR}}^{-1}\boldsymbol{\phi}\left(f_{dt},f_{st}\right), \tag{33}$$

where $\overline{\boldsymbol{\gamma}} = (1/M)\sum_{i=1}^{M}\boldsymbol{\gamma}_i$ is the averaged value of all the columns and

$$\begin{aligned}&\boldsymbol{\Omega}(f_{st}, f_{dt})\\&\quad=\left\{(p,q)\mid \left|f_{dp}-f_{dt}\right|\le\delta_d,\ \left|f_{sq}-f_{st}\right|\le\delta_s\right\}\end{aligned}\tag{34}$$

is the possible Doppler and spatial frequency domain including the assumed signal of interest (SOI), which can be determined by the rough a priori information for the target. The constants $\delta_d = \mu_d\Delta_d$ and $\delta_s = \mu_s\Delta_s$ reflect the tolerance to the uncertainty of the target normalized Doppler frequency and spatial frequency, where Δ_d and Δ_s are the discretizing resolutions determined by N_s and N_d, respectively. μ_d and μ_s are appropriate tolerance constants aiming to avoid target self-canceller.

In conclusion, the main procedure can be done as follows.

Step 1. By employing the guidelines of the BCS approach for dealing with complex data, the matrix $\widehat{\mathbf{X}}$ can be acquired and then vectorized as vector $\mathbf{y}$; according to (16) and $\boldsymbol{\Psi} = \widehat{\boldsymbol{\Phi}}\otimes\mathbf{I}_M$, we can transform the MMV model to the block SMV model.

Step 2. Initialize the parameter $\mathbf{B} = \mathbf{I}$ and solution vector $\mathbf{x}$.

Step 3. An iterative procedure is produced by learning rules (28), (29), and (31), resulting in updating the parameters ρ_n, $\mathbf{B}$, and λ.

Step 4. By (27) and (29), the mean value $\boldsymbol{\mu}_{\mathbf{x}}$ (the maximum a posteriori (MAP) estimate of $\mathbf{x}$) and variance $\boldsymbol{\Sigma}_{\mathbf{x}}$ can be computed.

Step 5. The procedure ends when the iterations reach the max times or the threshold of two adjoint iterations reaches some certain value. If not, go on with Steps 3 and 4.

Step 6. Output the value $\boldsymbol{\gamma} = [\boldsymbol{\gamma}_1, \boldsymbol{\gamma}_2, \ldots, \boldsymbol{\gamma}_M] \in \mathbb{C}^{N_sN_d\times M}$, estimate the parameter $\overline{\boldsymbol{\gamma}}$ using the secondary measurements via $\overline{\boldsymbol{\gamma}} = (1/M)\sum_{i=1}^{M}\boldsymbol{\gamma}_i$, and compute the clutter covariance matrix as (32).

Step 7. Design the STAP filter weights according to (33) and calculate the filter output $\mathbf{y} = \mathbf{w}_{\mathrm{SR}}^{H}\mathbf{x}$, where $\mathbf{x}$ is the received signal in the CUT. The target detection can be followed by binary hypothesis testing to determine the target presence (H_1) or absence (H_0), given by $\mathbf{y} \underset{\mathrm{H}_0}{\overset{\mathrm{H}_1}{\gtrless}} \boldsymbol{\varepsilon}$, where $\boldsymbol{\varepsilon}$ is the threshold scalar.

4. Experimental Results and Performance Analysis

In this section, simulations are conducted to demonstrate the effectiveness of the proposed method. The proposed simulated scenarios have the following parameters: $N = M = 10$, $d_R = d_T = 0.115$ m, pulse number $K = 10$, radar wavelength $\lambda = 0.23$ m, PRF $f_r = 2434.8$, platform velocity $v_p = 140$ m/s, platform height $H = 6000$ m, target velocity $v_r = 28$ m/s, target range 42 km, target azimuth 90°, clutter-to-noise ratio (CNR) 60 dB, and signal-to-noise ratio (SNR) 15 dB. The number of discretizing grids for the spatial frequency equals 50; that is, $N_s = N_d = 50$.

4.1. Spectrum Estimation Performance. The accuracy of clutter space-time spectrum estimation has a great impact on the ultimate clutter suppression performance. In this subsection, the spectrum estimation of the clutter and target with the methods below is examined. For FOCUSS algorithm, the stopping condition is decided by the criterion times, which is set to be 250. According to [9, 15], sparsity of clutter is $N+K-1 = 19$. As the spectrum including target, the sparsity corresponding to the criterion times is at least 20 for OMP algorithm.

Figure 2 shows the space-time spectrum estimated by SR-STAP algorithm and MIMOSR-STAP algorithm with only one snapshot. Figures 2(a) and 2(b) are obtained exploiting FOCUSS class algorithms [18, 21]. Figures 2(c) and 2(d) are obtained exploiting OMP class algorithms [17, 22]. Figures 2(e) and 2(f) are obtained exploiting SBL class algorithms [20, 23]. The results show that MIMOSR-STAP obtains more accurate clutter spectrum than SR-STAP, that is to say, different from the phased array radar; MIMOSR-STAP can be utilized to implement the joint sparse recovery of clutter spectrum in multiple snapshots of single range cell case. Figures 2(b), 2(d), and 2(f) show that our proposed method can obtain a clearer clutter spectrum with much less estimation error existing, such as clutter spectrum disconnection and "pseudopeaks." And that means our method can improve the accuracy of CCM estimation.

4.2. Performance Improvement. In this subsection, the improvement factor (IF) performance of the abovementioned methods is examined. Moreover, traditional methods such as STAP based on sample matrix inverse (SMI) algorithm and direct data domain (D3) algorithm are chosen to be the reference with comparing the standards. The training samples requirement of SMI-STAP algorithm is 200 (2NK). The subarray numbers of channel and pulse of D3 STAP algorithm are 4. The signal-to-clutter-plus-noise ratio (SCNR) is commonly used to assess the detection performance of airborne radar systems. Improvement factor (IF) is defined as the ratio of output SCNR to input SCNR:

$$\begin{aligned}\mathrm{IF} &= \frac{\mathrm{SCNR}_{\mathrm{out}}}{\mathrm{SCNR}_{\mathrm{in}}} = \frac{\boldsymbol{\omega}^{\mathbf{H}}\mathbf{S}\mathbf{S}^{\mathbf{H}}\boldsymbol{\omega}/\boldsymbol{\omega}^{\mathbf{H}}\left(\mathbf{R}_{\mathbf{C}}+\mathbf{R}_{\mathbf{N}}\right)\boldsymbol{\omega}}{\mathbf{S}^{\mathbf{H}}\mathbf{S}/\mathrm{tr}\left(\mathbf{R}_{\mathbf{C}}+\mathbf{R}_{\mathbf{N}}\right)}\\&= \frac{\boldsymbol{\omega}^{\mathbf{H}}\mathbf{S}\mathbf{S}^{\mathbf{H}}\boldsymbol{\omega}\cdot\mathrm{tr}\left(\mathbf{R}_{\mathbf{C}}+\mathbf{R}_{\mathbf{N}}\right)}{\boldsymbol{\omega}^{\mathbf{H}}\mathbf{S}\mathbf{S}^{\mathbf{H}}\boldsymbol{\omega}\mathbf{S}^{\mathbf{H}}\mathbf{S}},\end{aligned}\tag{35}$$

where tr(·) is matrix trace.

Figures 3(a) and 3(b) compare the IF performance of the proposed method using TMSBL [20] algorithm with MIMOSR-STAP using MFOCUSS [21], MOMP [22], SR-STAP using FOCUSS [18], OMP [17], SBL [23], SMI-STAP [24], and D3-STAP [24]. The IF performance of the SMI-STAP method is used as a theoretically optimal result, owing to which CCM estimation meets 2NK IID samples in simulated scenario. The D3-STAP does not require the

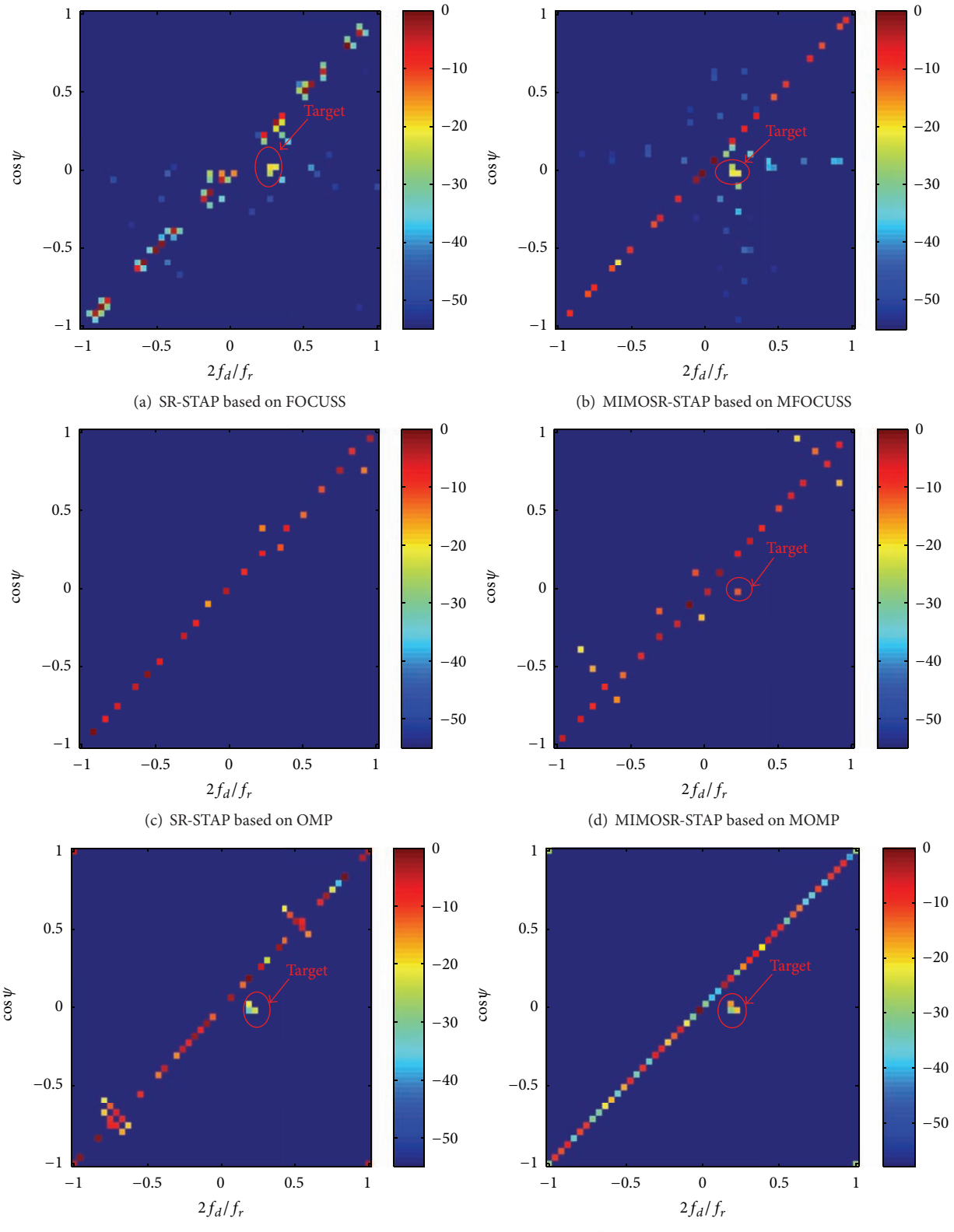

(a) SR-STAP based on FOCUSS

(b) MIMOSR-STAP based on MFOCUSS

(c) SR-STAP based on OMP

(d) MIMOSR-STAP based on MOMP

(e) SR-STAP based on SBL

(f) MIMOSR-STAP based on TMSBL

Figure 2: Spectrum estimation performance.

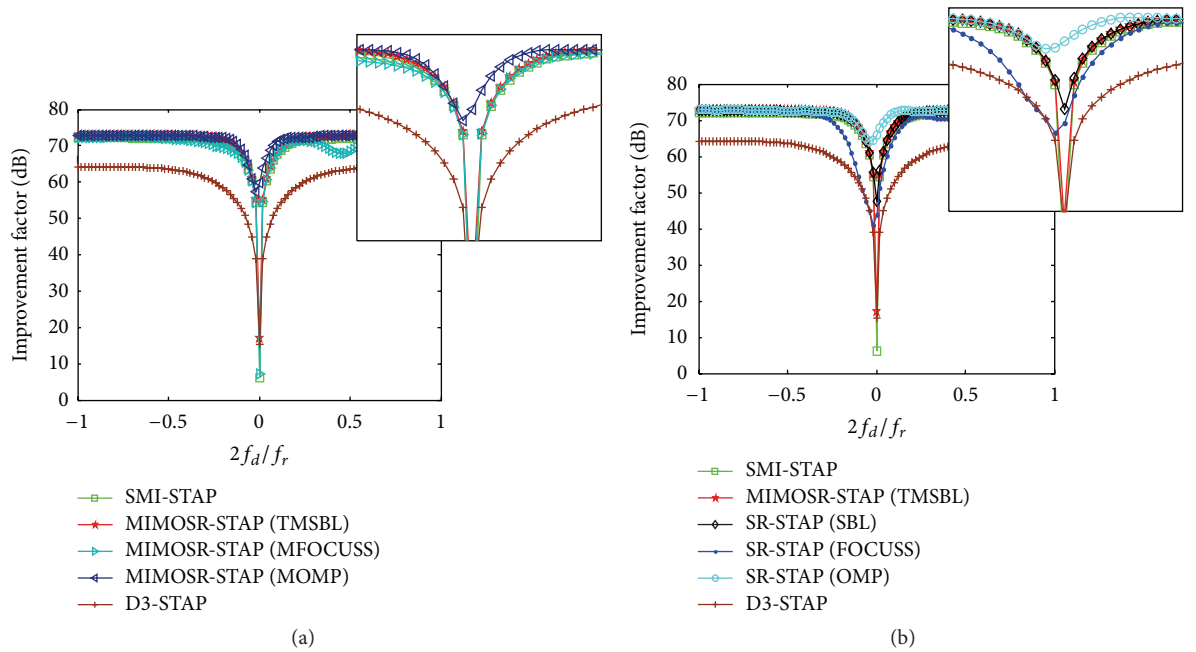

Figure 3: Improvement factor.

training data at the cost of reduced subaperture. The performance of D3-STAP declines because its system DOF decreases. Consistent with Figure 2, the proposed method outperforms other methods significantly and its performance is extremely close to the optimal method. Obviously, our proposed method can estimate the high-resolution space-time spectrum with one snapshot. Therefore, the proposed method's clutter covariance matrix (CCM) estimation is effective and results in good clutter suppression performance.

5. Conclusions

In this paper, a novel STAP algorithm for airborne MIMO radar based on Temporally Correlated Multiple Sparse Bayesian Learning (TMSBL) to mitigate heterogeneous clutter is studied. By exploiting the waveform diversity of MIMO radar, the cell under test can be transformed into multisnapshots for phased array radar, which seeks to estimate the high-resolution space-time spectrum with multiple measurement vectors. As a result, the proposed method suppresses clutter effectively. Compared with algorithms based on single measurement vector, MFOCUSS and MOMP, the proposed method could achieve better performance with only one snapshot, especially suitable for the seriously heterogeneous clutter environment which is difficult for catching independent and identically distributed (IID) training samples.

Competing Interests

The authors declare that they have no competing interests.

Acknowledgments

This work was supported in part by the National Natural Science Foundation of China (no. 61501501 and no. 61501504).

References

[1] R. Klemm, *Principles of Space-Time Adaptive Processing*, Institute of Electrical Engineering, London, UK, 3rd edition, 2006.

[2] W. L. Melvin, "A STAP overview," *IEEE Aerospace & Electronic Systems Magazine*, vol. 19, no. 1, pp. 19–35, 2004.

[3] J. R. Guerci and E. J. Baranoski, "Knowledge-aided adaptive radar at DARPA: an overview," *IEEE Signal Processing Magazine*, vol. 23, no. 1, pp. 41–50, 2006.

[4] R. Klemm, "Adaptive airborne MTI: an auxiliary channel approach," *IEE Proceedings F*, vol. 134, no. 3, pp. 269–276, 1987.

[5] H. Wang and L. Cai, "On adaptive spatial-temporal processing for airborne surveillance radar systems," *IEEE Transactions on Aerospace and Electronic Systems*, vol. 30, no. 3, pp. 660–670, 1994.

[6] W. Feng, Y. Zhang, X. He, and Y. Guo, "Cascaded clutter and jamming suppression method using sparse representation," *Electronics Letters*, vol. 51, no. 19, pp. 1524–1526, 2015.

[7] G. Ginolhac, P. Forster, F. Pascal, and J.-P. Ovarlez, "Performance of two low-rank STAP filters in a heterogeneous noise," *IEEE Transactions on Signal Processing*, vol. 61, no. 1, pp. 57–61, 2013.

[8] G. Ginolhac, P. Forster, F. Pascal, and J. P. Ovarlez, "Exploiting persymmetry for low-rank Space Time Adaptive Processing," *Signal Processing*, vol. 97, pp. 242–251, 2014.

[9] L. E. Brennan, J. Mallett, and I. S. Reed, "Theory of adaptive radar," *IEEE Transactions on Aerospace and Electronics Systems*, vol. 9, no. 2, pp. 237–251, 1973.

[10] Z. Yang, R. Fa, Y. Qin, X. Li, and H. Wang, "Direct data domain sparsity-based STAP utilizing subaperture smoothing techniques," *International Journal of Antennas and Propagation*, vol. 2015, Article ID 171808, 10 pages, 2015.

[11] S. F. Cotter, B. D. Rao, K. Engan, and K. Kreutz-Delgado, "Sparse solutions to linear inverse problems with multiple measurement vectors," *IEEE Transactions on Signal Processing*, vol. 53, no. 7, pp. 2477–2488, 2005.

[12] K. Sun, H. Zhang, G. Li et al., "A novel STAP algorithm using sparse recovery technique," in *Proceedings of the IEEE International Geoscience and Remote Sensing Symposium (IGARSS '09)*, vol. 5, pp. 336–339, Cape Town, South Africa, July 2009.

[13] K. Sun, H. Meng, Y. Wang, and X. Wang, "Direct data domain STAP using sparse representation of clutter spectrum," *Signal Processing*, vol. 91, no. 9, pp. 2222–2236, 2011.

[14] Z. Yang, R. C. de Lamare, and X. Li, "L1-Regularized STAP algorithms with a generalized sidelobe canceler architecture for airborne radar," *IEEE Transactions on Signal Processing*, vol. 60, no. 2, pp. 674–686, 2012.

[15] Z. Yang, X. Li, H. Wang, and W. Jiang, "On clutter sparsity analysis in space-time adaptive processing airborne radar," *IEEE Geoscience and Remote Sensing Letters*, vol. 10, no. 5, pp. 1214–1218, 2013.

[16] D. L. Donoho, M. Elad, and V. N. Temlyakov, "Stable recovery of sparse overcomplete representations in the presence of noise," *IEEE Transactions on Information Theory*, vol. 52, no. 1, pp. 6–18, 2006.

[17] J. A. Tropp and A. C. Gilbert, "Signal recovery from random measurements via orthogonal matching pursuit," *IEEE Transactions on Information Theory*, vol. 53, no. 12, pp. 4655–4666, 2007.

[18] I. F. Gorodnitsky and B. D. Rao, "Sparse signal reconstruction from limited data using FOCUSS: a re-weighted minimum norm algorithm," *IEEE Transactions on Signal Processing*, vol. 45, no. 3, pp. 600–616, 1997.

[19] D. P. Wipf and B. D. Rao, "Sparse Bayesian learning for basis selection," *IEEE Transactions on Signal Processing*, vol. 52, no. 8, pp. 2153–2164, 2004.

[20] Z. Zhang and B. D. Rao, "Sparse signal recovery with temporally correlated source vectors using sparse Bayesian learning," *IEEE Journal on Selected Topics in Signal Processing*, vol. 5, no. 5, pp. 912–926, 2011.

[21] R. Zdunek and A. Cichocki, "Improved M-FOCUSS algorithm with overlapping blocks for locally smooth sparse signals," *IEEE Transactions on Signal Processing*, vol. 56, no. 10, pp. 4752–4761, 2008.

[22] J. Chen and X. Huo, "Theoretical results on sparse representations of multiple-measurement vectors," *IEEE Transactions on Signal Processing*, vol. 54, no. 12, pp. 4634–4643, 2006.

[23] G. Oliveri and A. Massa, "Bayesian compressive sampling for pattern synthesis with maximally sparse non-uniform linear arrays," *IEEE Transactions on Antennas and Propagation*, vol. 59, no. 2, pp. 467–481, 2011.

[24] Y. Wang and Y. Peng, *Space-Time Adaptive Processing*, Tsinghua University Press, Beijing, China, 2000.